Applied Geochemistry 27 (2012) 1821–1828

Contents lists available at SciVerse ScienceDirect

Applied Geochemistry

journal homepage: www.elsevier.com/locate/apgeochem

Geochemistry of a continental saline aquifer for CO_2 sequestration: The Guantao formation in the Bohai Bay Basin, North China

Zhonghe Pang [a,*], Yiman Li [a,b], Fengtian Yang [a,b], Zhongfeng Duan [a,b]

[a] Key Laboratory of Engineering Geomechanics, Institute of Geology and Geophysics, Chinese Academy of Sciences, Beijing 100029, China
[b] Graduate School, Chinese Academy of Sciences, Beijing 100039, China

ARTICLE INFO

Article history:
Available online 3 March 2012

ABSTRACT

The Neogene Guantao formation in the Beitang sag in the Bohai Bay Basin (BBB) of North China, a Mesozoic–Cenozoic sedimentary basin of continental origin, has been chosen as a candidate for a pilot field test of CO_2 sequestration. Hydrogeological and geochemical investigations have been carried out to assess its suitability, taking advantage of many existing geothermal wells drilled to 2000 m or greater depths. Water samples from 25 wells and drill cores of three sections of the Guantao formation were collected for measurements of mineralogy, water chemistry and isotopes ($\delta^{18}O$, δD, $\delta^{13}C$, ^{14}C). Formation temperature estimated by chemical geothermometry is in the range of 60–80 °C. Geochemical modeling of water–rock–CO_2 interaction predicts a strong geochemical response to CO_2 injection. Besides the elevated porosity (33.6–38.7%) and high permeability (1150–1980 mD) of the Ng-III formation and a favorable reservoir–caprock combination, it is also found that the formation contains carbonates that will react with CO_2 after injection. The low salinity (TDS < 1.6 g/L) offers high CO_2 solubility. The ^{14}C age of the formation water indicates a quasi-closed saline aquifer system over large time scales, the lateral sealing mechanism for CO_2 sequestration requires further investigation. The CO_2 storage capacity of the Guantao formation within the Beitang sag is estimated to be 17.03 Mt, assuming pure solubility trapping.

1. Introduction

Global warming and frequent drought and flooding events have made anthropogenic emissions of CO_2 a global concern. The concentration of CO_2 in the atmosphere has risen from 280 ppm before the Industrial Era (1750s) to about 380 ppm at the present day (IPCC, 2005). A possible option to reduce CO_2 emission from industrial sources is to capture and dispose it in geological structures including depleted oil and gas fields, unminable coal beds and deep saline aquifers (Gunter et al., 1997; Pruess et al., 2003; Emberley et al., 2004; Shafeen et al., 2004; Benson, 2006; Kharaka et al., 2006; Gaus, 2009).

Due to their high storage capacity and wide availability, deep saline aquifers found in sedimentary basins have proven to be the most promising choice for CO_2 sequestration. The global CO_2 storage capacity of saline aquifers has been estimated to be from 350 Gt to 10,000 Gt (IPCC, 2005), which is >90% of the total space available underground. The CO_2 can be more effectively sequestrated in geological formations at pressures higher than 7.34 MPa (equivalent depth of about 800 m), and at temperatures above 31.1 °C, where CO_2 will stay in a supercritical state with an elevated density up to 600 kg/m^3, 400 times more condensed compared to that at atmospheric conditions.

The injected CO_2 can be sequestrated in deep saline aquifers through a combination of physical and chemical trapping mechanisms, which include stratigraphic or structural trapping, residual trapping, solubility trapping, mineral trapping and hydrodynamic trapping (Pruess et al., 2003; Xu et al., 2003; Moore et al., 2005; Wigand et al., 2008; Gilfillan et al., 2009; Michael et al., 2010). Once injected into a saline aquifer, CO_2 will move and spread slowly due to pressure gradients and gravitational effects as supercritical fluid or free-phase CO_2 and displace the groundwater in its flow domain. Such mechanisms are called hydrodynamic trapping. Residual trapping refers to part of the CO_2 trapped in much smaller pore spaces by capillary forces. Chemical trapping takes place when CO_2 dissolves in the formation water (solubility trapping) and water–rock–CO_2 interactions cause mineral trapping, which is the most stable and permanent way of CO_2 sequestration. However, mineral trapping comprises an insignificant portion, especially in the early stages after CO_2 injection. Although considerable effort has been made in understanding CO_2 trapping mechanisms, there are still many unsolved issues. Different trapping mechanisms would result in different CO_2 storage capacity estimates (IPCC, 2005; Audigane et al., 2007; Zhang et al., 2009).

Several commercial scale projects of CO_2 sequestration in deep saline aquifers (e.g. Sleipner, Snøhvit, Alberta acid gas injection, In

* Corresponding author.
E-mail address: z.pang@mail.iggcas.ac.cn (Z. Pang).

0883-2927/$ - see front matter © 2012 Elsevier Ltd. All rights reserved.
doi:10.1016/j.apgeochem.2012.02.017

Salah) and pilot field tests of CO_2 injection (e.g. Frio, Nagaoka, Ketzin, Gorgon) have demonstrated the technological feasibility of CO_2 sequestration (Emberley et al., 2004; Kharaka et al., 2006; Saito et al., 2006; Iding and Ringrose, 2009; Schilling et al., 2009; Rutqvist et al., 2009).

A typical small-scale pilot field test is that in the Frio sandstone formation in Texas, USA, where 1600 tones of supercritical CO_2 ($SCCO_2$) were injected to investigate the behavior of $SCCO_2$ in the formation, including geochemical reactions and physical processes of the CO_2 plume (Hovorka et al., 2006; Kharaka et al., 2006). An example of commercial scale CO_2 sequestration in deep saline aquifer is the Sleipner project in the North Sea, Norway, where one million tons of CO_2 has been injected each year into the Utsira formation at the off shore natural gas fields since 1996 (Maldal and Tappel, 2004). Geophysical and geochemical monitoring have not detected any CO_2 leakage so far (Arts et al., 2004). Both of the above cases are targeted at sedimentary basins of marine origin, where salinity is very high starting from that of seawater and formation mineralogy is relatively uniform and aquifer pore space heterogeneity is less pronounced.

Besides the field tests, laboratory experiments and numerical simulation of CO_2 migration and water–rock–CO_2 interactions are also being increasingly applied (IPCC, 2005; Kharaka et al., 2006; Gysi and Stefánsson, 2008; Mito et al., 2008).

Most of the deep saline aquifers in Chinese sedimentary basins that are close to emission sources, i.e. the Cenozoic sedimentary basins on the eastern coast of China, are filled with continental sediments, which make them behave differently from the marine sedimentary basins already tested and studied in other countries in terms of water chemistry evolution, matrix mineralogy, and aquifer heterogeneity. In particular, water–rock interaction processes are expected to be different and this has not been well understood.

Being one of the most typical sedimentary basins in eastern coastal China, the Bohai Bay Basin (BBB) is a potential candidate for CO_2 sequestration. Deep saline aquifers are widely distributed with a high CO_2 storage capacity. The Neogene Guantao formation of Beitang sag, Huanghua Depression, near the center of the BBB has been chosen as the test site for CO_2 injection to study water–rock–CO_2 interaction processes, trapping mechanisms and other related issues, including CO_2 plume migration, environmental impacts due to possible CO_2 leakage and long-term monitoring parameters. There is also a possibility of using the off-shore extension of the same aquifer. Once successfully tested on-shore, commercial scale storage can probably be implemented off-shore.

The purpose of this paper is to discuss water–rock CO_2 interaction processes anticipated for a saline aquifer of continental origin through hydrogeological and geochemical investigation of the reservoir–caprock system, including water and drill core sample collection and analyses as well as chemical thermodynamic modeling.

2. Study area

As one of the industrial centers in North China, the Tianjin area is facing major challenges regarding CO_2 emission reduction compared to other areas in the country. Carbon dioxide emission is mainly from coal-burning power plants. Carbon dioxide sequestration in deep saline aquifers is considered as a viable option because the aquifers are widely distributed in the BBB. The Guantao formation composed of Neogene continental sediments is among the most promising formations to serve as a reservoir for storage.

In order to study geochemical processes involved after CO_2 is injected so as to understand the trapping mechanisms and to address safety issues associated with CO_2 sequestration, section III in the lower part of the Guantao formation in the Beitang sag near the center of the BBB was chosen (Fig. 1).

The study area is located in the Tanggu District of Tianjin Binhai New Area, where the Guantao formation has been the major aquifer for geothermal energy development to supply heat and hot water for space heating and recreation purposes in the past decades (Dong et al., 2004; Ma et al., 2006; Hu et al., 2007). Abundant geological and hydrogeological data is available and wells are available to collect water and drill core samples for water–rock interaction investigations.

3. Geology of the Beitang Sag

The BBB is a large Mesozoic–Cenozoic intracratonic sedimentary basin filled by continental sediments of Paleocene, Neogene and Quaternary ages. The sedimentary center is in the Bohai Bay area. The Beitang sag is located in the western side of the central part of the BBB, which is bordered by the Hangu fault to the north, by the Cangdong fault to the west, by the Haihe fault to the south and by the Bohai Bay to the east (Fig. 1). Details of stratigraphic features are shown in Figs. 2 and 3 (location of A–A′ cross section is marked in Fig. 1).

Quaternary clay and sandstone sediments are widely distributed in the study area at variable depths from 0 m to more than 520 m, composed of clay and sandy clay. The Neogene Minghuazheng and Guantao formations lie unconformably above the highly folded, Mesozoic to Precambrian crystalline basement (Fig. 3). The Minghuazheng formation overlies the Guantao formation at a depth of about 1300 m and is composed of mudstone and sandy mudstone of variable thickness, interbedded with sandstone. Regional electrical conductivity values are 2–7 Ω m. The extensive Quaternary and Neogene Minghuazheng formations are considered excellent cap-rock layers to prevent CO_2 from escaping after being injected into the Guantao formation.

In the Beitang sag, the thickness of the Guantao formation is from 350 m in the west to about 550 m in the east. It is composed of a series of red fluvial sandstone units with distinct sedimentary cycles. From top to bottom, three sub sections, i.e. Ng-I, Ng-II and Ng-III are distinguished with the Ng-III as the intended aquifer for CO_2 sequestration. The Ng-III is composed of sandstone, sandy gravel and gravel while Ng-II represents a thin layer of mudstone, serving as an immediate cap-rock seal.

Drill cutting samples show that the local mudstone zone of the Ng-II formation contains pyrite. According to XRD analysis of drill core samples from the Guantao formation, the reservoir rock is mainly composed of quartz, feldspar (including albite and anorthite), montmorillonite, illite, kaolinite and minor chlorite. Total chemical analysis shows that the rock is mainly composed of

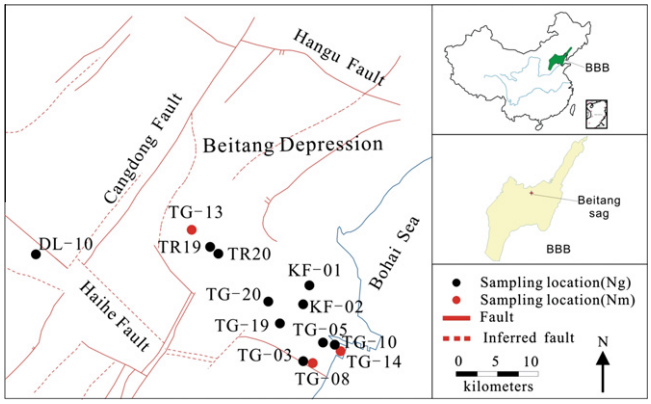

Fig. 1. Location of the study area and distribution of sampled wells from the Beitang sag in the Bohai Bay Basin (Ng: Guantao formation, Nm: Minghuazheng formation).

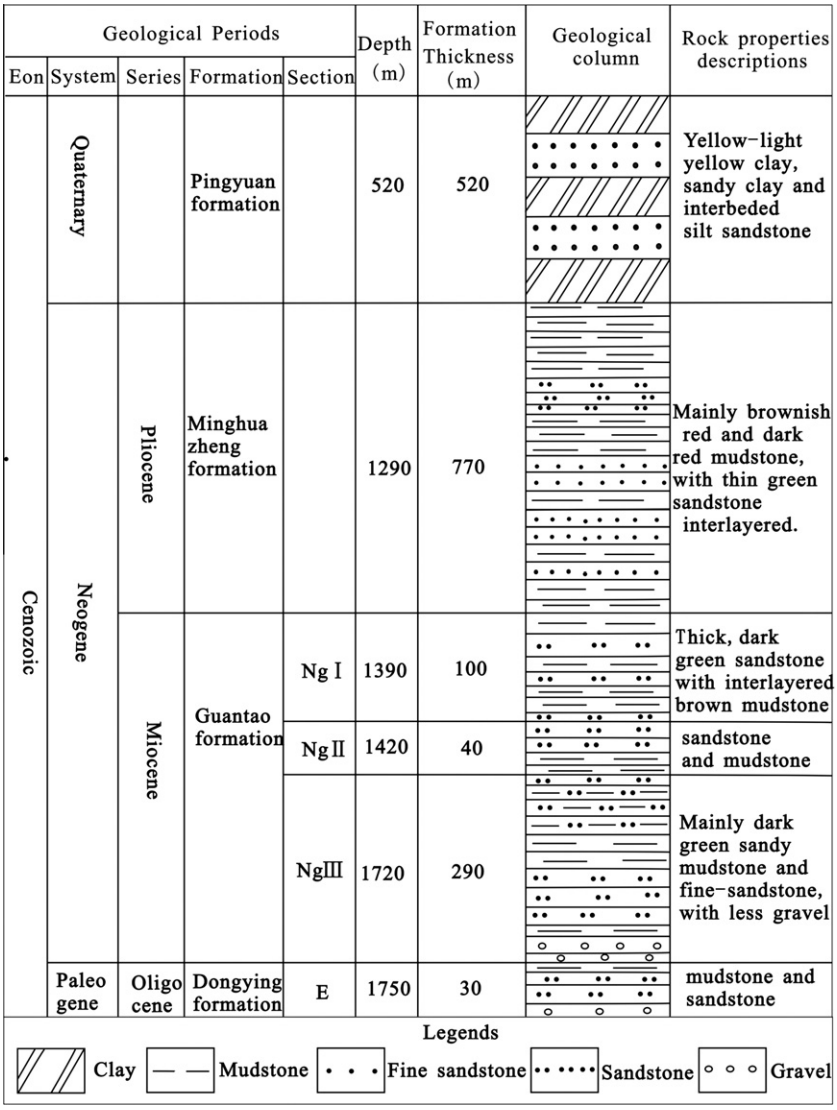

Fig. 2. The stratigraphic column of well TR20 in the Beitang sag.

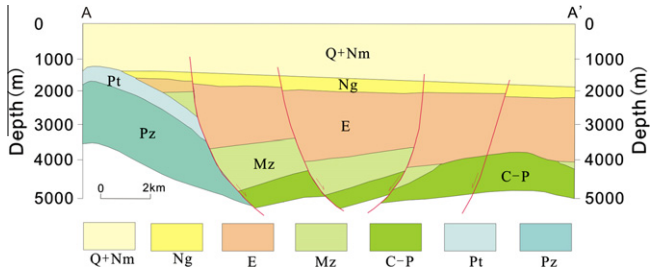

Fig. 3. (A–A′) Cross-section of the Beitang sag. Q: Quaternary, Nm: Neogene Minghuazheng formation, Ng: Neogene Guantao formation, E: Eocene, C–P: Carboniferous and Permian, Pt: Proterozoic, Pz: Paleozoic, Mz: Mesozoic.

silica and alumina (about 69.4 wt.% and 11.9 wt.%, respectively, Table 1). The Fe_2O_3 and CaO are 3.2% and 2.5%, respectively.

Based on logging data from geothermal wells, the permeability of sandstone in the Guantao formation varies from 1.165 to 2.003 μm^2 (about 1150–1980 mD), while the porosity is 33.6–38.7%. These values are considered as indicative for favorable conditions for CO_2 sequestration and provide opportunities for the study of geochemical processes (solubility trapping and mineral trapping mechanisms). Compared to the underlying Eocene strata, Guantao is a reservoir with elevated porosity and permeability and lower salinity characteristics, and a more economic depth range. The cross-section in Fig. 3 shows that the Guantao formation has a regional extension, offering flexibility in terms of avoiding conflicts with other underground resource utilization schemes.

The Beitang sag is tectonically located in the northern part of the Huanghua depression of the BBB. There are two main fault systems in the area with NNE and NWW oriented alignments, including the Haigu fault in the north, Cangdong fault in the west and the Haihe fault in the south. The Cangdong fault is a major regional fault system that was formed during the Mesozoic period and reactivated in Cenozoic. It controls the distribution of the Guantao formation to a certain extent. The Haihe fault extends into the Bohai Sea towards the east and serves as a tectonic boundary between the Beitang and the Banqiao sags. The Hangu normal fault located on the northern border of the Beitang sag controlled sedimentation during Mesozoic and Paleocene periods. The planned CO_2 injection well is located near Haihe fault and possible leakage from this fault will be monitored to assess any possible impacts on environmental safety.

Table 1
Total chemical analysis of reservoir rock (Ng) in the Beitang sag (in wt.%).

Sample ID	SiO_2	TiO_2	Al_2O_3	Fe_2O_3	MnO	MgO	CaO	Na_2O	K_2O	P_2O_5	LOI	FeO	Total
Ng-I	76.34	0.27	11.13	2.26	0.03	1.09	1.23	2.48	2.73	0.09	1.94	1.02	99.59
Ng-II	76.82	0.24	10.93	2.09	0.03	1.34	1.32	2.23	2.32	0.06	2.40	0.95	99.78
Ng-III	55.08	0.67	13.55	5.21	0.08	5.48	4.99	1.58	2.68	0.12	10.52	2.42	99.96

4. Sampling and analyses

Several sampling campaigns were implemented in December 2009 and May 2010, during which water samples were collected from 24 geothermal production wells, with depths from 1400 m to 2100 m, including 19 from the Neogene Guantao formation and five from the overlying Minghuazheng formation in the Beitang sag. Chemical and isotopic analyses have been completed. The locations of the sampled wells are shown in Fig. 1.

For cation analysis, samples were acidified with HNO_3 to adjust pH to less than 2. For dissolved CO_2 and HCO_3^-, titration with 0.05 M NaOH and 0.02 M HCl were carried out *in situ*. Dissolved inorganic C in the water was collected using the $SrCl_2$ precipitation method *in situ*. Some physical and chemical parameters like pH, temperature, conductivity, Eh and dissolved O_2 as well as Fe(II) were determined in the field, using a multi parameter device HACH Sension 156. Samples were filtered using a 0.45 μm membrane in the laboratory before analysis.

Chemical analysis of the water samples was performed in the Analytical Laboratory of the Beijing Research Institute of Uranium Geology. Main anions (F^-, Cl^-, SO_4^{2-} and NO_3^-) were determined using a DIONEX-500 ion chromatograph and HCO_3^- by a 785DMP titrator and cations with an OPTIMA2X00/1500 ICP-OES, trace elements by ICP-MS, all within one week of sampling.

Stable isotopes ($\delta^{18}O$, δD, $\delta^{13}C$) and ^{14}C were determined in the Water Isotope and Water–Rock Interaction Laboratory, and Stable Isotope Laboratory and Cosmogenic Isotope Laboratory at the Institute of Geology and Geophysics, Chinese Academy of Sciences (IGG-CAS). $\delta^{18}O$ and δD values were determined with a laser absorption water isotope analyzer Picarro L1102-I, $\delta^{13}C$ ratios by MAT253 isotope mass spectrometer and ^{14}C using the benzene preparation and liquid scintillation counting measurement.

In addition, three drill core samples from the Guantao formation were collected from a new borehole in the sag and analyzed for major and minor mineral and chemical components by XRD and XRF in the IGG-CAS.

5. Hydrochemistry of the Guantao and Minghuazheng aquifers

5.1. Formation water chemistry

Water samples collected from the Guantao formation Ng-III aquifer are of HCO_3·Cl–Na or Cl·HCO_3–Na type. The TDS (Total Dissolved Solids) concentration is from 1.15 g/L to 1.65 g/L (Table 2), which is favorable for CO_2 sequestration because lower salinity means higher CO_2 solubility in formation water. The wellhead temperatures measured are mostly between 50 °C and 70 °C with three wells below 50 °C. pH determined *in situ* indicates that the water is neutral to alkaline with an average pH of 7.7. As shown in the Piper diagram (Fig. 4), formation water is dominated by Na^+, HCO_3^- and Cl^- ions and the average concentrations are 496.6 mg/L, 605.3 mg/L and 310.8 mg/L, respectively, while Ca^{2+} and Mg^{2+} ion concentrations are low. The F^- concentration is from 3.9 mg/L to 9.6 mg/L with an average of 6.3 mg/L, while Si ranges from 30 to 48 mg/L with an average value of 37.8 mg/L.

Average concentrations of the trace elements Li, Sr, Ba and Cr are 1.2 mg/L, 0.76 mg/L, 0.084 mg/L and 0.156 mg/L, respectively. Metals like Cu, Zn, Mn and Pb are generally depleted in the water.

As a comparison, reservoir temperature and TDS in the water samples of the Minghuazheng formation are lower than those for the Guantao formation. The average temperature is 45.5 °C and TDS is from less than 1 g/L to about 1.3 g/L and water chemistry is uniformly of HCO_3–Na type (Table 2, Fig. 4).

Table 2
Chemical and isotopic analyses of formation water in Guantao (Ng) and Minghuazheng (Nm) formations (pH_f: pH measured *in situ*). Concentration of major elements in mg/L.

Sample ID	Formation	T (°C)	pH_f	F	Cl	NO_3	SO_4	HCO_3	Ca	Mg	Na	K	SiO_2	$\delta^{18}O$ (‰)	δ^2H (‰)	$\delta^{13}C$ (‰)	^{14}C (pmc)	TDS (g/L)
TG08	Nm	40.4	8.2	3.2	52.1	0.1	53.4	596	5.1	0.8	309.0	4.5	22.0	−9.26	−73.0	−13.1		0.75
TG10	Nm	46	8.4	4.3	21.2	0.0	28.2	669	4.6	0.7	293.0	4.1	25.9	−10.00	−72.4	−13.4		0.72
TG13	Nm	43	8.6	4.0	85.1	0.8	73.8	590	10.0	2.0	300.0	11.8	29.8	−9.36	−72.6	−11.6		0.81
DL20	Nm	51	8.2	5.7	300.8	3.3	205.5	513	24.0	7.8	434.0	44.0		−8.82	−73.4			1.28
DL31	Nm	47	8.0	5.4	296.5	1.4	200.9	560	26.0	8.1	439.0	44.0		−8.87	−71.4			1.30
DG49	Ng	58	8.2	7.7	605.4	0.8	181.2	559	18	7.5	579	44		−7.54	−68.0			1.72
DL10	Ng	62	7.2	7.2	316.6	1.3	202.8	610	34.3	6.8	467.0	39.2	29.9	−9.38	−73.3	−6.1	12.79	1.42
DL25	Ng	73	7.0	9.6	336.6	0.0	228.2	530	60.0	17.5	503.0	98.0		−8.30	−73.6			1.52
HX38	Ng	53.5	7.9	3.9	221.5	0.6	320.4	455	45.0	6.9	418.0	44.0		−9.46	−72.2		7.58	1.29
JN02	Ng	64	7.4	8.3	423.3	0.0	240.1	616	47.0	6.7	534.0	70.0		−9.10	−72.1		1.74	1.64
KF01	Ng	60	7.7	5.3	225.5	1.3	163.2	645	11.6	0.9	477.0	10.0	39.8	−9.64	−71.8	−7.4	12.2	1.26
KF02	Ng	66	7.6	6.9	258.0	0.1	175.3	635	10.9	0.9	496.0	9.8	39.7	−9.95	−71.1	−6.8	14.65	1.32
TG03	Ng	72	8.0	5.8	305.8	1.5	191.6	645	12.0	1.0	531.0	11.4	43.4	−9.18	−72.0	−8.9	12	1.43
TG05	Ng	70	7.4	5.7	315.5	1.1	220.5	641	12.7	1.0	546.0	10.1	40.7	−9.21	−72.7	−7.1	10.48	1.47
TG14	Ng	70	7.6	4.9	272.7	2.2	172.0	670	10.8	1.1	519.0	11.5	48.0	−9.45	−72.2	−8.9	11.24	1.38
TG18	Ng	60	7.7	6.4	284.6	1.2	196.9	620	12.9	1.3	491.0	10.4	38.6	−9.08	−71.0	−7.2	14.9	1.35
TG19	Ng	63	7.5	6.7	324.8	1.1	208.6	651	14.0	1.4	557.0	10.9	38.8	−8.90	−72.2	−6.5	9.09	1.49
TG20	Ng	63	7.4	4.5	277.4	1.5	184.7	641	14.7	1.4	509.0	10.5	37.1	−9.16	−72.6	−5.9	10.76	1.36
TG24	Ng	46.4	7.6	5.6	204.9	1.0	143.9	613	23.1	4.8	397.0	32.1	33.5	−9.40	−72.9	−8.0	10.72	1.15
TG38	Ng	66	7.9	6.0	273.3	0.4	205.4	673	14.0	7.0	476.0	45.0		−9.24	−72.2			1.36
TGR28	Ng	64	8.4	6.5	359.8	0.9	240.6	479	11.8	0.8	502.6	3.5	38.0					1.65
TR19	Ng	54	7.7	6.2	258.8	0.0	173.7	611	18.8	3.1	465.0	17.7	33.0	−9.36	−73.3	−6.4	7.1	1.28
TR19B	Ng	36	7.7	6.9	356.7	0.8	233.6	602	19.5	3.2	523.0	18.0	34.9	−9.34	−72.1			1.50
TR20	Ng	36	7.8	5.2	283.4	1.5	182.9	606	19.0	3.1	444.0	18.0	33.3	−9.43	−73.1			1.29

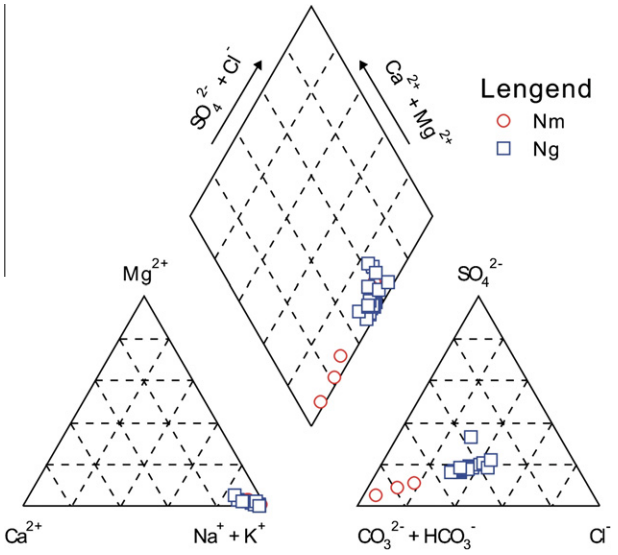

Fig. 4. Piper diagram of Neogene formation waters from the Beitang sag. The red open-circles represent water samples collected from the Minghuazheng formation while blue open-squares those from the Guantao formation. (For interpretation of the references to color in this figure legend, the reader is referred to the web version of this article.)

5.2. Isotope geochemistry and age of formation water

5.2.1. Isotope composition of formation water

$\delta^{18}O$ values of the Guantao formation water fall within a range from −7.5‰ to −10.0‰ (VSMOW) and δD values from −68.0‰ to −73.4‰ (Table 2, Fig. 5). Compared to the Guantao formation, the Minghuazheng formation shows a similar trend with −8.8‰ to −9.3‰ (VSMOW) and −71.4‰ to −73.0‰, for $\delta^{18}O$ and δ^2H, respectively.

Stable isotope ratios for the water samples indicate their meteoric origin. Guantao formation waters show a slight positive $\delta^{18}O$ shift by 2.5‰ in the ^2H vs. ^{18}O plot (Fig. 5). This positive $\delta^{18}O$ shift has also been observed in low temperature geothermal waters in other sedimentary basins in China. In the Xi'an geothermal field of the Guanzhong basin, the O shift amounts to as much as 10‰, where the formation temperature is from 40 °C to 90 °C (Qin et al., 2005). This has been interpreted as being caused by water–rock interaction with carbonate rocks in the formation matrix (Pang et al., 2010a,b).

5.2.2. $\delta^{13}C$ isotope and ^{14}C age of the formation water

The average $\delta^{13}C$ value of the Minghuazheng formation water is −12.7‰, while that of the Guantao formation is −7.2‰ (Table 2, Fig. 6). The fact that the $\delta^{13}C$ of the Minghuazheng formation is very different from that of the Guantao formation implies that there is little hydraulic connection between both formations.

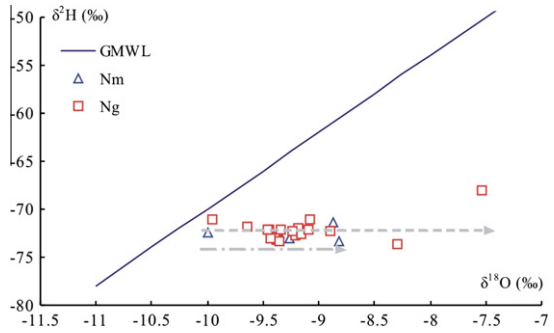

Fig. 5. Hydrogen and oxygen isotope ratios in Neogene formation waters from the Beitang sag.

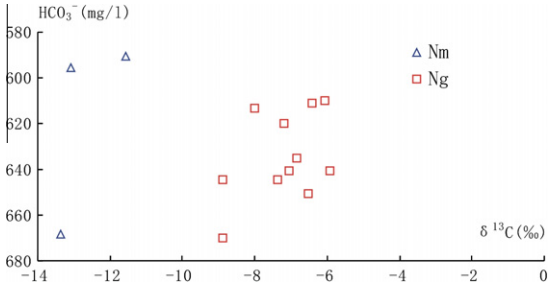

Fig. 6. Plot of $\delta^{13}C$ vs. HCO_3^- of geothermal water from the Guantao and Minghuazheng formation, Beitang sag, Bohai Bay Basin, North China.

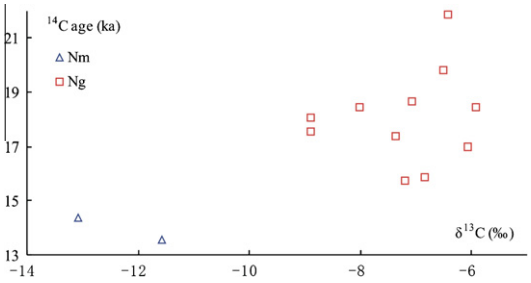

Fig. 7. Plot of $\delta^{13}C$ vs. ^{14}C age of geothermal water from the Guantao and Minghuazheng aquifers, Beitang sag, Bohai Bay Basin, North China.

The HCO_3^- and $\delta^{13}C$ relationship is a good indicator for the origin of carbonates in water. For the Minghuazheng formation, soil carbonate dominates due to its shallower location and younger age, as compared to Guantao formation, which gets its HCO_3^- mainly from the formation matrix (Fig. 6).

The ^{14}C-age of Guantao formation water offers further evidence for the discussions above. The age of Guantao formation water is positively related to its $\delta^{13}C$ values (Fig. 7), which shows that longer residence time allows more $\delta^{13}C$ enrichment as more carbonate is dissolved from the formation matrix and there is less input of atmospheric CO_2 (Pang et al., 2010a). The ^{14}C-residence time of Guantao formation water ranges from 13.5 to 21.9 ka (Fig. 7), a quasi-closed and tight underground environment for CO_2 sequestration.

5.3. Modeling water–rock–CO_2 interaction

In order to study the geochemical response of the Guantao formation to CO_2 injection, thermodynamic modeling of water–rock–CO_2 interaction has been carried out using PHREEQC V2.15 software with the wateq4f.dat thermodynamic database (Parkhurst and Appelo, 1999). Since the hydrogeochemistry of Guantao formation water is quite uniform (for details see Table 2), a water sample from well TR19 and drill core samples from the Guantao formation in the southeastern Beitang sag were selected as representatives for the aquifer.

To simplify the modeling process, pressure influence and kinetic aspects of minerals involved were not considered and the measured wellhead temperature of 54 °C was adopted. The model referred to 1 kg of water and 0.01 mol of rock reacting with injected CO_2 under the five different scenarios of 9.68, 14.24, 27.82, 69.92 and 196.8 mmol, respectively, resulting in partial pressures or fugacity (P) of CO_2 (g) of the saline water to be 10^{-1}, $10^{-0.5}$, 1, $10^{0.5}$, 10 bar accordingly (Li et al., 2010).

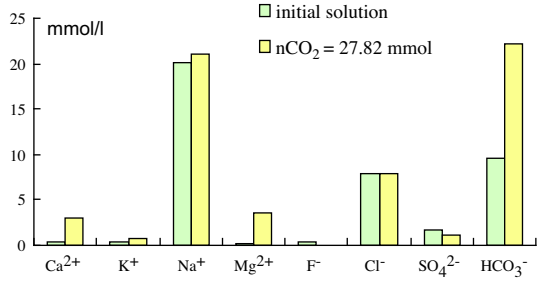

Fig. 8. Chemical compositional changes at nCO_2 = 27.82 mmol ($P_{CO2(g)}$ = 1 bar).

Modeling the injection of 27.82 mmol CO_2 caused a pH decrease by about 1.5 pH units due to CO_2 dissolution. Simultaneously, Al and Si concentrations increased from 0 and 0.55 mmol/L to 5.1 mmol/L and 12.4 mmol/L, respectively, due to the dissolution of Al-bearing silicate minerals (Fig. 8). Concentrations of conservative species, including Cl^-, NO_3^- remained constant while Na^+ slightly increased. The Ca^{2+}, Mg^{2+} and HCO_3^- concentrations increased, especially HCO_3^- by 12.6 mmol/L. Compared with the original formation water, calcite and dolomite were over-saturated. Quartz and chalcedony became more over-saturated because of silicate mineral dissolution and the formation of secondary minerals such as dawsonite.

This trend of water chemistry change is in agreement with previous modeling, experiments and field tests (Kharaka et al., 2006). When CO_2 is injected into the reservoir, it will first be dissolved in the water, which will later decompose to H^+ and HCO_3^-. Water–rock interaction will be accelerated as carbonate and aluminosilicate minerals will dissolve and secondary minerals (e.g. dawsonite) will be formed. However, an increase of Fe was not observed in the present simulation, which may be attributed to the lack of Fe-bearing minerals (Kharaka et al., 2006; Mito et al., 2008).

6. Temperature and pressure conditions in the formation

Reservoir temperature (T) and pressure (P) conditions are important parameters for potential CO_2 sequestration sites as CO_2 will be in a supercritical state when $T \geqslant 31.1$ °C and $P \geqslant 7.38$ MPa. Temperature and pressure conditions of the Guantao formation have been established using well logging curves from geothermal well completion reports in the Beitang Sag. The average temperature and pressure gradients were found to be 3.74 °C/100 m and 1.03 MPa/100 m, respectively (Ma et al., 2006) (Fig. 9). Drilling data for geothermal wells in the Beitang sag indicate that the Guantao formation is composed of a series of red sandstone units with depth ranging from 1300 m to 1850 m deep. Injected CO_2 would stay in supercritical state in this depth range.

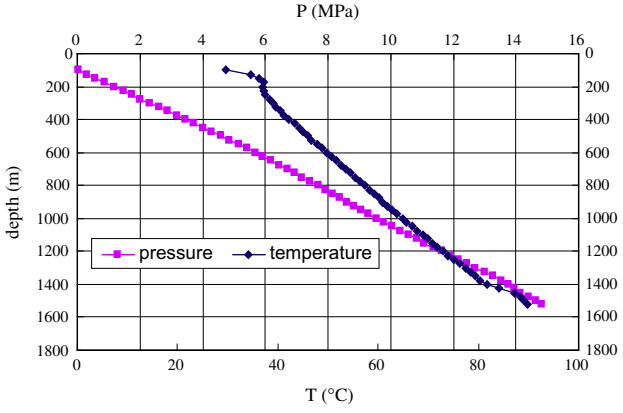

Fig. 9. Subsurface temperature and pressure gradients for the Beitang sag, Bohai Bay Basin.

Table 3
Measured and calculated reservoir temperatures.

Code	Ts (°C)	Na–K	Na–K–Ca	Quartz	Chalcedony
TG08	40.4	55.4	106.3	52.3	38.5
TG05	70	65.1	115.9	78.4	63.8
TG03	72	71.5	121.9	81.4	66.7
TG20	63	69.7	119.8	74.3	59.7
TG19	63	67.5	118.0	76.3	61.7
TG14	70	72.9	123.3	86.1	71.3
TG10	46	53.9	104.9	58.9	44.9
KF02	66	67.7	118.2	77.3	62.7
KF01	60	70.4	120.6	77.4	62.8
TG18	60	70.9	121.0	76.0	61.4
TG24	46.4	141.3	181.8	69.8	55.4
TG13	43	100.2	146.4	64.8	50.5
TR19	54	98.5	145.5	69.1	54.7

Ts: Sampling temperature at the wellhead. Geothermometers and their references are: Na–K (Giggenbach, 1988), quartz (Fournier, 1977), chalcedony (Arnórsson et al., 1983) and Na–K–Ca (Fournier and Truesdell, 1973).

Based on the analysis of geophysical data and drilling information, the injection well in the Guantao formation has inflow zones at depths from 1350 m to 1718 m. Temperature at the wellhead is 60 °C and downhole pressure is about 15 MPa. Since CO_2 solubility in formation water is in function with the reservoir temperature, pressure and salinity, reservoir temperature conditions were estimated using established chemical geothermometers (Table 3).

According to previous experience in the region, the actual reservoir temperatures are usually higher than those measured at the wellhead by 10–15 °C. Low chalcedony geothermometers are considered to be unrealistic, and cation geothermometers are generally not reliable in this kind of low temperature environment due to non-equilibrium with feldspars and clay minerals due to kinetic effects. The Quartz geothermometer temperatures are considered representative of typical reservoir temperature with a range between 50 and 90 °C in the formation.

7. Storage capacity assessment

Carbon dioxide can be sequestrated in deep saline aquifers through a combination of physical and chemical trapping mechanisms, including structural and stratigraphic, residual, solubility, and mineral trapping and integrated hydrodynamic trapping (IPCC, 2005).

When CO_2 is injected into a deep saline aquifer, it will first move due to pressure and gravitational gradients and a part of it will dissolve in the formation water. The gravity segregation and fingering phenomena will affect the sweep efficiency (Ef), which depends on the reservoir permeability, thickness and mobility ratio of the injected CO_2 and the properties of the formation water (Tanaka et al., 1995; Xu et al., 2006; Zhang et al., 2011). The solubility of CO_2 in the formation water is controlled by salinity (TDS), reservoir temperature and pressure, whereby solubility increases with increasing pressure and decreasing salinity and temperature.

Several CO_2 capacity assessment methods have been developed based on these trapping mechanisms which involve a wide range of uncertainties because of the complexity and variations of these trapping mechanisms during CO_2 migration and dissolution processes (Bachu and Adams, 2003; Li et al., 2004; Bachu et al., 2007; Bradshaw et al., 2007; Ogawa et al., 2009; Takahashi et al., 2009; Vangkilde-Pedersen et al., 2009).

There is no widely accepted standard method for storage capacity assessment. Tanaka and coworkers set up two models based on underground structures (Tanaka et al., 1995; Takahashi et al.,

Table 4
Reservoir parameters of the Beitang sag for CO_2 capacity calculations.

Parameters	Reservoir information
Rock type	Sandstone
Density of CO_2 at standard conditions (ρ)	1.977 kg/m^3
Storage factor (Sf)	0.5
Effective formation thickness (h)	450 m
Storage area (A)	2.03×10^9 m^2
Porosity (Φ)	36%

2009). Model (1) is configured to be applied to aquifers in anticlinal structures and model (2) to aquifers in monoclinal structures on land and 100% solubility trapping. Since the Guantao formation can be treated as aquifers in monoclinal structures on land, model (2) has been adopted for CO_2 capacity calculation here.

$$MCO_2 = Ef \cdot A \cdot h \cdot \Phi \cdot \rho \cdot [Sg/Bg(CO_2) + (1 - Sg)Rs(CO_2)] \quad (1)$$

$$MCO_2 = Sf \cdot A \cdot h \cdot \Phi \cdot Rs(CO_2) \cdot \rho \quad (2)$$

where Ef is the sweep efficiency (fraction, dimensionless), A is storage area (m^2), h is effective formation thickness (m), Φ is effective reservoir porosity (fraction, dimensionless), Sg is saturation of supercritical CO_2 (fraction, dimensionless), $Bg(CO_2)$ is CO_2 formation volume factor (m^2/m^3, reservoir volume/standard volume), $Rs(CO_2)$ is CO_2 solubility in formation water (m^3/m^3), ρ is density of CO_2 at standard conditions (kg/m^3) and Sf is the storage factor (fraction, dimensionless)

These are essential parameters in CO_2 capacity calculations, some of which depend on empirical data. Capacity estimates for the Beitang sag are partly based on measured parameters on reservoir porosity, permeability, stratum thickness and spreading area. Carbon dioxide solubility in formation water is calculated according to a theoretical model from Duan and Sun (2003) and Duan et al. (2006). The parameters used to calculate storage capacity are listed in Table 4.

The porosity of the Guantao formation, measured in drill cores ranges from 33.6% to 38.7% with an average value of 36% used. The effective formation thickness is estimated to be 450 m. A spreading area of 2030 km^2 was adopted (Deng et al., 2006). The density of CO_2 at standard conditions is 1.977 kg/m^3 and a CO_2 solubility of 0.05239 kg/kg at formation conditions was calculated based on a salinity of 0.15%, temperature of 54 °C and pressure of 15 MPa. The storage factor was assumed to be 0.5 for the Guantao formation according to the literature (Tanaka et al., 1995; Shafeen et al., 2004; Ogawa et al., 2009; Takahashi et al., 2009). A more accurate capacity assessment will rely on detailed geological information of the target formation and numerical simulations should be carried out. Using the parameters (Table 4) and the model (2) presented above, the CO_2 storage capacity of the Beitang Sag is estimated to be 17.03 Mt.

8. Conclusions

A hydrogeological and geochemical characterization has been carried out on the Neogene Guantao formation in the BBB, North China, focusing on the Beitang sag in Tianjin area. It is a sedimentary basin filled with continental sediments that is rather different from previous studies but typical for Chinese sedimentary basins.

A good combination of reservoir (sand aquifers with high porosity and permeability) and cap-rock features (multi clay layers with great thickness and low permeability) is confirmed. Water chemistry with low salinity, elevated porosity and permeability of the host formation, low to medium temperature, and pressure ranges offers favorable conditions for CO_2 sequestration. The isotopic composition of Guantao formation water suggests the presence of carbonate in the host rock so strong water–rock interaction within the reservoir is expected which may result in changes of formation porosity and permeability after CO_2 injection.

The residence time based on ^{14}C in Guantao formation water indicates that the formation is a quasi-closed system on large time scales and the role of regional groundwater in CO_2 sequestration requires further investigation in terms of lateral sealing mechanisms. Results from geochemical modeling of water–rock–CO_2 interaction show that the injection of CO_2 will induce similar changes in water chemistry to those observed in previous tests (Cantucci et al., 2009; Kharaka et al., 2006) except for Fe that is missing in the system. Integrating geochemical information with other parameters such as porosity and effective thickness, the CO_2 storage capacity of the Guantao formation at the Beitang sag is estimated to be 17.03 Mt, assuming 100% solubility trapping.

Overall, the site is considered suitable for a CO_2 sequestration pilot test with emphasis on geochemical responses and hydrodynamic effects. The geochemical information can be used for planning post-injection monitoring operations. Fault systems are developed in the study area, so possible leaks along these natural conduits should be further investigated.

Acknowledgements

This study was financially supported by the China National High-Tech R&D (863) Program (Grant No. 2208AA062303). Part of the work was presented as a keynote lecture at the 13th WRI-Symposium in Guanajuato, Mexico, August 2010. The authors benefited from discussions with Yousif Kharaka at the early stage of the work. Halldor Armannsson and an anonymous reviewer are thanked for their constructive comments that have helped to improve the quality of the paper. Thanks are also due to Peter Birkle for his patience and guidance in the editorial handling of this special issue.

References

Arnórsson, S., Gunnlaugsson, E., Svavarsson, H., 1983. The chemistry of geothermal waters in Iceland. III. Chemical geothermometry in geothermal investigations. Geochim. Cosmochim. Acta 47, 567–577.

Arts, R., Eiken, O., Chadwick, A., Zweigel, P., van der Meer, B., Kirby, G., 2004. Seismic monitoring at the Sleipner underground CO_2 storage site (North Sea). Geol. Soc. Lond. Spec. Publ. 233, 181–191.

Audigane, P., Gaus, I., Czernichowski-Lauriol, I., Pruess, K., Xu, T., 2007. Two-dimensional reactive transport modeling of CO_2 injection in a saline aquifer at the Sleipner site, North Sea. Am. J. Sci. 307, 974–1008.

Bachu, S., Adams, J.J., 2003. Sequestration of CO_2 in geological media in response to climate change: capacity of deep saline aquifers to sequester CO_2 in solution. Energy Convers. Manage. 44, 3151–3175.

Bachu, S., Bonijoly, D., Bradshaw, J., Burruss, R., Holloway, S., Christensen, N.P., Mathiassen, O.M., 2007. CO_2 storage capacity estimation: methodology and gaps. Int. J. Greenhouse Gas Contr. 1, 430–443.

Benson, S.M., 2006. Monitoring CO_2 sequestration in deep geological formations for inventory and carbon credits. In: SPE Ann. Technical Conf. Exhibition, 24–27, Texas, USA.

Bradshaw, J., Bachu, S., Bonijoly, D., Burruss, R., Holloway, S., Christensen, N.P., Mathiassen, O.M., 2007. CO_2 storage capacity estimation: issues and development of standards. Int. J. Greenhouse Gas Contr. 1, 62–68.

Cantucci, B., Montegrossi, G., Vaselli, O., Tassi, F., Quattrocchi, F., Perkins, E.H., 2009. Geochemical modeling of CO_2 storage in deep reservoirs: the Weyburn project (Canada) case study. Chem. Geol. 265, 181–197.

Deng, R.J., Xu, B., Qi, J.F., Zhang, L.X., Wang, D.L., Yang, H., 2006. Sedimentation characteristics and factors affecting the reservoir in Palaeogene Shasan Member of Beitang sag, Huanghua depression. Acta Petrol. Min. 25, 230–236 (in Chinese).

Dong, J., Li, C., Wang, K., 2004. Geothermal Resources Exploration and Utilization Planning Technology Report. Tianjin Geothermal Exploration and Development-Designing Institute (in Chinese).

Duan, Z., Sun, R., 2003. An improved model calculating CO_2 solubility in pure water and aqueous NaCl solutions from 273 to 533 K and from 0 to 2000 bar. Chem. Geol. 193, 257–271.

Duan, Z., Sun, R., Zhu, C., Chou, I.M., 2006. An improved model for the calculation of CO_2 solubility in aqueous solutions containing Na^+, K^+, Ca^{2+}, Mg^{2+}, Cl^-, and SO_4^{2-}. Mar. Chem. 98, 131–139.

Emberley, S., Hutcheon, I., Shevalier, M., Durocher, K., Gunter, W.D., Perkins, E.H., 2004. Geochemical monitoring of fluid–rock interaction and CO_2 storage at the Weyburn CO_2-injection enhanced oil recovery site, Saskatchewan, Canada. Energy Convers. Manage. 29, 1393–1401.

Fournier, R.O., 1977. Chemical geothermometers and mixing models for geothermal systems. Geothermics 5, 41–50.

Fournier, R.O., Truesdell, A.H., 1973. An empirical Na–K–Ca geothermometer for natural waters. Geochim. Cosmochim. Acta 37, 1255–1275.

Gaus, I., 2009. Role and impact of CO_2–rock interactions during CO_2 storage in sedimentary rocks. Int. J. Greenhouse Gas Contr. 4, 73–89.

Giggenbach, W.F., 1988. Geothermal solute equilibria. Derivation of Na–K–Mg–Ca geoindicators. Geochim. Cosmochim. Acta 52, 2749–2765.

Gilfillan, S.M.V., Sherwood Lollar, B., Holland, G., Blagburn, D., Stevens, S., Schoell, M., Cassidy, M., Ding, Z., Zhou, Z., Lacrampe-Couloume, G., Ballentine, C.V., 2009. Solubility trapping in formation water as dominant CO_2 sink in natural gas fields. Nature 458, 614–618.

Gunter, W.D., Wiwchar, B., Perkins, E.H., 1997. Aquifer disposal of CO_2-rich greenhouse gases: Extension of the time scale of experiment for CO_2-sequestering reactions by geochemical modelling. Mineral. Petrol. 59, 121–140.

Gysi, A.P., Stefánsson, A., 2008. Numerical modelling of CO_2–water–basalt interaction. Mineral. Mag. 72, 55–59.

Hovorka, S.D., Benson, S.M., Doughty, C., Freifeld, B.M., Sakurai, S., Daley, T., Kharaka, Y.K., Holtz, M.H., Trautz, R.C., Seay Nance, H., Myer, L.R., Knauss, K.G., 2006. Measuring permanence of CO_2 storage in saline formations: the Frio experiment. Environ. Geosci. 13, 105–121.

Hu, Y., Lin, L., Zhao, S. 2007. Sustainable Exploration Potential Assessment Report of Geothermal Resources in Tianjin city (in Chinese).

Iding, M., Ringrose, P., 2009. Evaluating the impact of fractures on the long-term performance of the In Salah CO_2 storage site. Energy Procedia 1, 2021–2028.

IPCC, 2005. In: Metz, B., Davidson, O., de Coninck, H.C., Loos, M., Meyer, L.A. (Eds.), IPCC Special Report on Carbon Dioxide Capture and Storage. Prepared by Working Group III of the Intergovernmental Panel on Climate Change. Cambridge University Press.

Kharaka, Y.K., Cole, D.R., Hovorka, S.D., Gunter, W.D., Knauss, K.G., Freifeld, B.M., 2006. Gas–water–rock interactions in Frio Formation following CO_2 injection: Implications for the storage of greenhouse gases in sedimentary basins. Geology 34, 577–580.

Li, X.C., Ohsumi, T., Koide, H., Akimoto, K., Kotsubo, H., 2004. Near-future perspective of CO_2 aquifer storage in Japan: site selection and capacity. Energy 30, 2360–2369.

Li, Y., Pang, Z., Yang, F., Duan, Z., 2010. Modelling the geochemical response of CO2 injection into the Guantao Formation, North China Basin. In: Birkle, P., Torres-Alvarado, I.S. (Eds.), Water–Rock Interaction 13. Proc. Internat Conf. WRI 13. CRC Press, Taylor & Francis Group, The Netherlands, pp. 875–878.

Ma, F., Lin, L., Cheng, W., Zhao, S., Zhao, S., 2006. Discussion on sustainable exploration and utilization of geothermal resources. Geol. Survey Res. 29, 222–228 (in Chinese).

Maldal, T., Tappel, I.M., 2004. CO_2 underground storage for Snøhvit gas field development. Energy 29, 1403–1411.

Michael, K., Golab, A., Shulakova, V., Ennis-King, J., Allinson, G., Sharma, S., Aiken, T., 2010. Geological storage of CO_2 in saline aquifers – a review of the experience from existing storage operations. Int. J. Greenhouse Gas Contr. 4, 659–667.

Mito, S., Xue, Z.Q., Ohsumi, T., 2008. Case study of geochemical reactions at the Nagaoka CO_2 injection site, Japan. Int. J. Greenhouse Gas Contr. 2, 309–318.

Moore, J., Adams, M., Allis, R., Lutz, S., Rauzi, S., 2005. Mineralogical and geochemical consequences of the long-term presence of CO_2 in natural reservoirs: An example from the Springerville-St. Johns Field, Arizona, and New Mexico, USA. Chem. Geol. 217, 365–385.

Ogawa, T., Shidahara, T., Nakanishi, S., Yamamoto, T., Yoneyama, K., Okumura, T., Hashimoto, T., 2009. Storage capacity assessment in Japan: comparative evaluation of CO_2 aquifer storage capacities across regions. Energy Procedia 1, 2685–2692.

Pang, Z., Yang, F., Huang, T., Duan, Z., 2010a. Genetic model of geothermal reservoirs in Guanzhong basin with implications to sustainable geothermal resources development. In: Proc. World Geothermal Congress, Bali, Indonesia, 25–29 April.

Pang, Z., Yang, F., Li, Y., Duan, Z., 2010b. Integrated CO2 sequestration and geothermal development: saline aquifers in the Beitang depresion, Tianjin, North China Basin. In: P. Birkle, P., Torres-Alvarado, I.S. (Eds.), Water-Rock Interaction 13. Proc. Internat Conf. WRI 13. CRC Press, Taylor & Francis Group, The Netherlands, pp. 31–36.

Parkhurst, D.L., Appelo, C.A.J., 1999. User's guide to PHREEQC (version 2) – a computer program for speciation, batch-reaction, one-dimensional transport, and inverse geochemical calculations. US Geol. Surv. Water-Resour. Invest. Rep. 99–4259.

Pruess, K., Xu, T.F., Apps, J., Garcia, J., 2003. Numerical modeling of aquifer disposal of CO_2. SPE J. 8, 49–60.

Qin, D.J., Turner, J.V., Pang, Z.H., 2005. Hydrogeochemistry and groundwater circulation in the Xi'an geothermal field, China. Geothermics 34, 471–494.

Rutqvist, J., Vasco, D.W., Myer, L., 2009. Coupled reservoir-geomechanical analysis of CO_2 injection at In Salah, Algeria. Energy Procedia 1, 1847–1854.

Saito, H., Nobuoka, D., Azuma, H., Xue, Z., Tanase, D., 2006. Time-lapse crosswell seismic tomography for monitoring injected CO_2 in an onshore aquifer, Nagaoka, Japan. Explor. Geophys. 37, 30–36.

Schilling, F., Borm, G., Würdemann, H., Möller, F., Kühn, M., 2009. Status report on the first European on-shore CO_2 storage site at Ketzin (Germany). Energy Procedia 1, 2029–2035.

Shafeen, A., Croiset, E., Douglas, P.L., Chatzis, I., 2004. CO_2 sequestration in Ontario, Canada. Part I: storage evaluation of potential reservoirs. Energy Convers. Manage. 45, 2645–2659.

Takahashi, T., Ohsumi, T., Nakayama, K., Koide, K., Miida, H., 2009. Estimation of CO_2 aquifer storage potential in Japan. Energy Procedia 1, 2631–2638.

Tanaka, S., Koide, H., Sasagawa, A., 1995. Possibility of underground CO_2 storage in Japan. Energy Convers. Manage. 36, 527–530.

Vangkilde-Pedersen, T., Anthonsen, K.L., Smith, N., Kirk, K., Neele, F., van der Meer, B., Le Gallo, Y., Bossie-Codreanu, D., Wojcicki, A., Le Nindre, Y.M., Hendriks, C., Dalhoff, F., Peter, Christensen.N., 2009. Assessing European capacity for geological storage of carbon dioxide – the EU GeoCapacity project. Energy Procedia 1, 2663–2670.

Wigand, M., Carey, J.W., Schütt, H., Spangenberg, E., Erzinger, J., 2008. Geochemical effects of CO_2 sequestration in sandstones under simulated in situ conditions of deep saline aquifers. Appl. Geochem. 23, 2735–2745.

Xu, T.F., Apps, J.A., Pruess, K., 2003. Reactive geochemical transport simulation to study mineral trapping for CO_2 disposal in deep arenaceous formations. J. Geophys. Res. 108 (B2), 2071. doi:10.1029/2002JB001979.

Xu, X., Chen, S., Zhang, D., 2006. Convective stability analysis of the long-term storage of carbon dioxide in deep saline aquifers. Adv. Water Resour. 29, 397–407.

Zhang, W., Li, Y., Xu, T., Cheng, H., Zheng, Y., Xiong, P., 2009. Long-term variations of CO_2 trapped in different mechanisms in deep saline formations: a case study of the Songliao Basin, China. Int. J. Greenhouse Gas Contr. 3, 161–180.

Zhang, W., Li, Y., Omambia, A.N., 2011. Reactive transport modeling of effects of convective mixing on long-term CO_2 geological storage in deep saline formations. Int. J. Greenhouse Gas Contr. 5, 241–256.